The motion of Brownian particles and sediment on an inclined plate

By A. A. DAHLKILD

Department of Mechanics, Royal Institute of Technology, 100 44 Stockholm, Sweden

The gravitational settling of a homogeneous suspension of Brownian particles on an inclined plate is considered. The hindered settling towards the wall and the viscous, buoyancy-driven bulk motion of the sediment are considered assuming steady conditions and accounting for the effects of Brownian diffusion, shear-induced diffusion and migration of particles due to a gradient in shear stress. Generally, the results show the development of a sediment boundary layer where the settling towards the wall is balanced by Brownian diffusion at the beginning of the plate and by shear-induced diffusion further downstream. Compared to previous results in the literature, the present theory allows steady-state solutions for extended values of the plate inclination and particle volume fraction above the sediment; upon reconsidering the case with non-Brownian particles, a new similarity solution, with a stable shock in particle density, is developed.

1. Introduction

An important task in separation technology is separation of the smallest biological factors – proteins, viruses, antibodies, vaccines, etc. These particles are so small that Brownian motion may affect the sedimentation process. In particular, the ability to transport and remove sedimented particles along the walls of a centrifuge or a gravity settling device will crucially depend on the degree of packing of the particles in the sludge layer. Gradient diffusion of particles due to Brownian motion is in this respect an advantage since it acts as to counteract the formation of high-particle-density layers. In addition, if the sediment layer is not stationary but flows along the wall, yet another diffusion mechanism is present due to the shearing motion of the suspending fluid. The self-diffusivity of particles in a shear flow was first measured by Eckstein, Baile & Shapiro (1977) by recurrent observations of a particular labelled particle of a homogeneous, neutrally buoyant suspension. Gadala-Maria (1979) made observations during shear of a suspension that was attributed to resuspension of a settled layer of buoyant particles. The increased diffusivity of a scalar rather than the particles themselves due to shearing of a suspension was addressed by Leal (1973). The phenomena of shear-induced diffusion of particles have more recently been studied extensively by Leighton & Acrivos (1986, 1987a, b), Schaflinger, Acrivos & Zhang (1990), Davis & Sherwood (1990), Chapman & Leighton (1991) and Acrivos, Mauri & Fan (1993). As variously described by these authors hydrodynamic interactions between particles, as they are advected by the fluid, results in a random walk and drift of particles perpendicular to the plane of shear. For particles of radius a in a fluid with shear rate $\dot{\gamma}$ the effective diffusivity of this mechanism scales as $a^2\dot{\gamma}$. The relative importance compared to Brownian diffusion is measured by the ratio $a^3\mu\dot{\gamma}/kT$ where μ is the dynamic viscosity of the suspending fluid.

Nir & Acrivos (1990, hereafter referred to as N & A), consider gravitational sedimentation and sediment flow on an inclined plate for the case of infinitely large values of $a^3\mu\dot{\gamma}/kT$, i.e. when Brownian motion is absent. They show that in a certain regime of the inclination angle and particle volume fraction far away from the plate, steady-state boundary layer solutions exist for the sediment flow down the plate. If the inclination angle is too small or the volume fraction is too small or too large, no steady-state solution was found with their theory since maximum packing of particles appeared at the wall and prevented the continuous transport of sediment. As pointed out by N & A, an odd feature of their solution is that for vanishing particle volume fraction in the suspension above the sediment, the thickness of the sludge layer grows indefinitely and no steady-state solution is possible whatever slope is given to the plate. Since for zero volume fraction there would be no sediment layer at all this seems counterintuitive. The authors attribute this puzzling result to the limitations of the model. One explanation could be (A. Nir 1996, private communication) that due to the dense packing of particles formed adjacent to the plate at low ambient volume fraction, the viscosity of the sediment is too high to allow any substantial shear rate development for diffusion of the particles. Also, consideration of the transient problem of a growing sediment layer would probably require progressively longer times to reach a steady state as the ambient volume fraction is decreased, suggesting that the limit of vanishing volume fraction results in a sediment of infinitesimal, increasing thickness. In a recent paper by Kapoor & Acrivos (1995, hereafter referred to as K & A), the inclusion of particle slip at the wall is also shown to eliminate this anomaly at the beginning of the plate, by which a plug of constant concentration slips along the inclined plate. Far from the leading edge, though, the slip velocity becomes weaker and eventually reduces to zero.

In the present paper we consider a more elaborate model which includes Brownian motion and, as recently also by K & A, a migration model for flows with shear stress gradients. These desired extensions eliminate the anomaly experienced by N & A in their case. Whereas most previous studies deal with flows for which $a^3\mu\dot{\gamma}/kT \gg 1$, the present paper considers Péclet numbers $a^3\mu\dot{\gamma}/kT \sim 1$. Close to the leading edge where the shear rate of the buoyancy-driven sediment-layer flow along the plate is weak, Brownian diffusion is actually completely dominant. Far downstream, however, the shear-induced diffusion of the accelerating sediment layer gradually takes over. The downstream scenario sketched above is not always true though. If the sediment gets sufficiently dense the shear rate close to the wall may be too small to suspend the particles even far downstream. Brownian diffusion is then the only mechanism left that prevents particles from attaining a state of maximum packing. The mechanism of particle migration due to shear stress gradients included in our model is frequently described in the literature (see e.g. Leighton & Acrivos 1987b; Koch 1989; Schaflinger 1994) but is not accounted for by N & A. Note that the existence of different regions along the plate, with various physical mechanisms emphasized, are also distinguished in the study by K & A described briefly in the previous paragraph, although in our case the picture is more complicated.

We also reconsidered the problem without Brownian motion. As the shear rate, and thereby also the diffusivity for this case, approach zero in the outer part of the sediment layer a shock in the particle volume fraction may form there. It was found that, for reasons of stability, the shock construction must be modified in order to recover that solution in the limit of vanishing Brownian motion for the extended formulation.

2. Formulation

The settling of spherical particles of radius a is assumed to take place above a semi-infinite two-dimensional flat plate at inclination angle ϕ to the horizontal as shown in figure 1. Far above the plate we have a well-mixed homogeneous suspension with constant particle volume fraction α_0. The distance to the upper interface of the suspension is infinitely large. We look for steady-state solutions of the 'mixture formulation' (see Ishii 1975) of two-phase flow. If the local volume fraction of particles is α, the density of the mixture is

$$\rho = \alpha\rho_D + (1-\alpha)\rho_C, \tag{2.1}$$

where subscripts C and D denote the separate, unmixed densities of the continuous and dispersed phases respectively. Let $\boldsymbol{j} = (j_x, j_y)$ and $\boldsymbol{q} = (u, v)$ denote volume-average and mass-averaged flux densities of the mixture, given by

$$\boldsymbol{j} = \boldsymbol{j}_D + \boldsymbol{j}_C, \quad \rho\boldsymbol{q} = \rho_D\boldsymbol{j}_D + \rho_C\boldsymbol{j}_C, \quad \boldsymbol{j}_D = \alpha\boldsymbol{v}_D, \quad \boldsymbol{j}_C = (1-\alpha)\boldsymbol{v}_C, \tag{2.2a–d}$$

where $\boldsymbol{v}_D$ and $\boldsymbol{v}_C$ are the separate velocities of the two phases, and let $\boldsymbol{j}_R$ denote the relative volume flux density of the dispersed phase defined by

$$\boldsymbol{j}_R = \boldsymbol{j}_D - \alpha\boldsymbol{j}. \tag{2.3}$$

It then follows that $\boldsymbol{j}$ and $\boldsymbol{q}$ are related by

$$\boldsymbol{j} = \boldsymbol{q} - \frac{\epsilon}{1+\epsilon\alpha}\boldsymbol{j}_R, \tag{2.4}$$

where ϵ is the relative density difference between the phases

$$\epsilon = (\rho_D - \rho_C)/\rho_C. \tag{2.5}$$

The mixture fluid is effectively assumed Newtonian with an empirical law for the relative viscosity as a function of the volume fraction of particles. Here, and subsequently throughout the paper, we follow the terminology of N & A as closely as possible and use

$$\frac{\mu}{\mu_C} = \mu_e(\alpha) = \left(1 + \frac{1.5\alpha}{1-\alpha/\alpha_m}\right)^2, \quad \alpha_m = 0.58. \tag{2.6}$$

For $\boldsymbol{j}_R$ we postulate a constitutive law according to

$$\boldsymbol{j}_R = \boldsymbol{j}_s + \boldsymbol{j}_{diff} + \boldsymbol{j}_{br}. \tag{2.7}$$

The first contribution is sedimentation due to gravity which for hindered settling based on Stokes' formula is given by

$$\boldsymbol{j}_s = \alpha f(\alpha)\,\boldsymbol{U}_s, \quad \boldsymbol{U}_s = \frac{2}{9}\frac{\rho_C\,\epsilon g a^2}{\mu_C}, \tag{2.8}$$

where $$f(\alpha) = (1-\alpha)/\mu_e(\alpha) \tag{2.9}$$

describes the hindering effect of the particles at finite volume fractions. The second term is diffusion of particles due to the mechanisms of shear-induced hydrodynamic
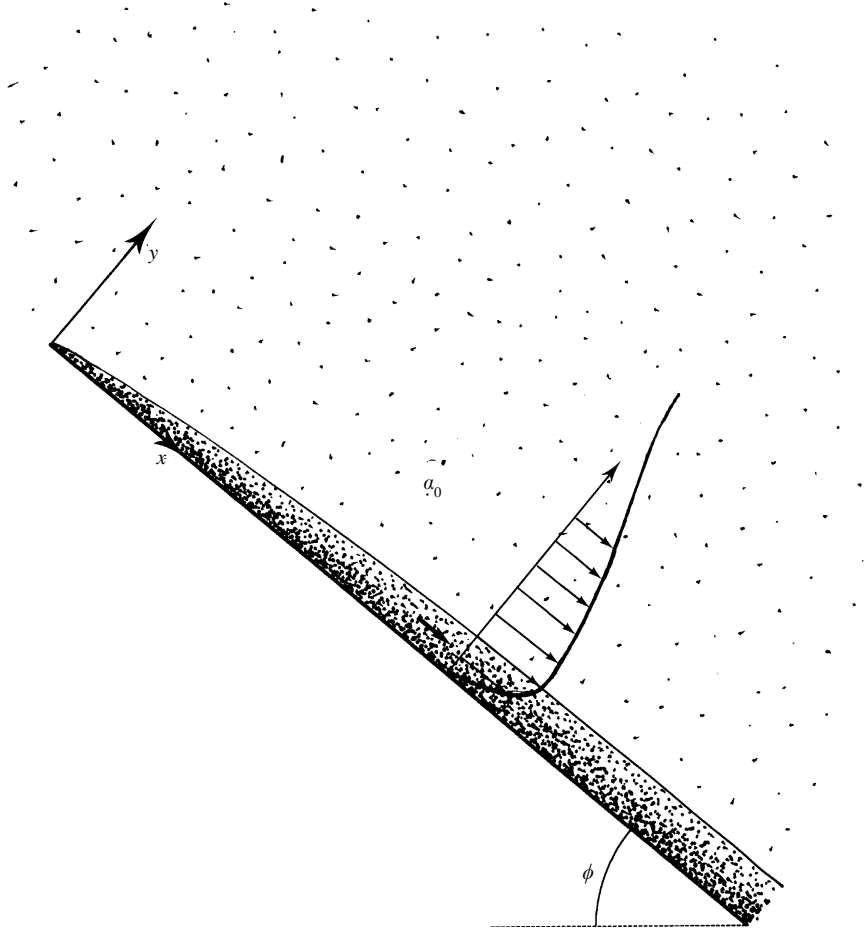
FIGURE 1. Geometry and coordinate system.

interaction in uni-directional flow as proposed in the literature. In addition to shear-induced gradient diffusion we include migration due to gradients in the shear stress, τ_{xy}, described by Leighton & Acrivos (1987b) and Schaflinger (1996), which yield

$$\boldsymbol{j}_{diff} = -\hat{\boldsymbol{y}}\left\{a^2\dot{\gamma}\beta(\alpha)\frac{\partial}{\partial y}\alpha + a^2\dot{\gamma}\kappa(\alpha)\frac{1}{\tau_{xy}}\frac{\partial}{\partial y}\tau_{xy}\right\}, \tag{2.10}$$

where $\dot{\gamma}$ is the shear rate. Approximate values of β and κ are

$$\alpha(\beta) = \tfrac{1}{3}\alpha^2(1+0.5\,\mathrm{e}^{8.8\alpha}), \quad \kappa(\alpha) = 0.6\,\alpha^2, \tag{2.11a, b}$$

as given by Leighton & Acrivos (1986, 1987b) and determined from curve fits to their experimental data. One may note that these data do not cover the range $\alpha > 0.5$ for which these coefficients, thus, are only speculative. The assumption of uni-directional particle diffusion applies approximately here since we consider only parameter regimes with a boundary layer character of the flow in the sediment layer.

The third term in (2.7) is gradient diffusion due to Brownian motion of the particles which is given by

$$\boldsymbol{j}_{br} = -D_C\,f(\alpha)\,\boldsymbol{\nabla}\Pi = -D_C\,f(\alpha)\,\Pi'(\alpha)\,\boldsymbol{\nabla}\alpha, \tag{2.12}$$

where $D_C = kT/6\pi\mu_C a$ is the Stokes–Einstein relation for the Brownian diffusivity in the dilute limit and $\Pi(\alpha)$ is the non-dimensional osmotic pressure of the suspension. Expressions for Π are given by Batchelor (1976) in the dilute limit:

$$\Pi_{dil}(\alpha) = \alpha(1 + 4\alpha + 10\alpha^2 + \ldots), \quad \alpha \ll 1, \tag{2.13}$$

and by Woodcock (1981) in the dense limit:

$$\Pi_{den}(\alpha) = \alpha\,\frac{1.85}{\alpha_m - \alpha}, \quad \alpha_m - \alpha \ll 1. \tag{2.14}$$

For our purpose it will be sufficient to use a straightforward combination of these limits in a formula for $\Pi'(\alpha)$;

$$\Pi'(\alpha) = \Pi'_{dil} + \Pi'_{den} - \frac{1.85}{\alpha_m}(1 + 2\alpha/\alpha_m + 3(\alpha/\alpha_m)^2). \tag{2.15}$$

The last three terms of (2.15) constitute the dilute-limit approximation of $-\Pi'_{den}$. Thus, (2.15) approaches the dilute-limit approximation for $\alpha \ll 1$ and also captures the singularity of the dense limit at $\alpha = \alpha_m$.

Note that, generally, the effective Brownian diffusivity of (2.12) would approach infinity as the volume fraction approaches maximum packing. However, the particular formula used for $f(\alpha)$ here coincidentally cancels the singular behaviour of Π', so that the effective Brownian diffusivity actually approaches a finite value at maximum packing of the particles. This seems to be a coincidence and of no physical significance. In fact, many other common formulas for the hindered settling function, $f(\alpha)$, do not cancel the singularity of Π' as for example $(1-\alpha)^{6.55}$ as used by Auzerais, Jackson & Russel (1988) in a similar model for transient settling of Brownian particles in one dimension. Therefore, in the expression for j_{br}, we make an exception and use

$$j_{br} = -D_C(1-\alpha)^2(1-\alpha/\alpha_m)^{2.5\alpha_m}\Pi'(\alpha)\,\nabla\alpha \tag{2.16}$$

(Ishii & Chawla 1979), instead of (2.12), whereas everywhere else $f(\alpha)$ is as given in (2.9). This procedure keeps our model identical to that of N & A in those parts where the same physical effect is described. Therefore, our results should vary from theirs only due to the new physical effects included, i.e. those of particle migration due to gradients in shear stress and Brownian diffusion.

Non-dimensional variables are introduced using U_s, ρ_C, μ_C, $\rho_C gL$ as typical values of velocity, density, viscosity and pressure and L is an, at present arbitrary, characteristic length of the plate.

Conservation of mixture and dispersed-phase volume and the momentum balance require respectively

$$\nabla\cdot j = \nabla\cdot q - \epsilon\nabla\cdot(j_R/(1+\epsilon\alpha)) = 0, \tag{2.17}$$

$$\nabla\cdot j_D = \nabla\cdot(\alpha j) + \nabla\cdot j_R = 0, \tag{2.18}$$

$$\frac{Re_L}{\Lambda_L}(1+\epsilon\alpha)\,q\cdot\nabla q = -\nabla P + (\alpha - \alpha_0)\hat{g} + \frac{1}{\Lambda_L}$$
$$\times\{\nabla\cdot[\mu_e(\alpha)(\nabla q + \nabla q^T)] - \nabla[\tfrac{2}{3}\mu_e(\alpha)\nabla\cdot q]\}, \tag{2.19}$$

where $P = p - (1+\epsilon\alpha_0)(x\cos\phi - y\sin\phi)$ is the reduced pressure,

$$j_R = \alpha f(\alpha)\hat{g} - \frac{1}{\Lambda_L}\frac{9}{2}\left|\frac{\partial u}{\partial y}\right|\left\{\beta(\alpha)\frac{\partial\alpha}{\partial y} + \kappa(\alpha)\frac{1}{\tau_{xy}}\frac{\partial\tau_{xy}}{\partial y}\right\}\hat{y} - \frac{1}{Pe_L}D(\alpha)\,\nabla\alpha \tag{2.20}$$

and
$$D(\alpha) = (1-\alpha)^2 \, (1-\alpha/\alpha_m)^{2.5\alpha_m} \, \Pi'(\alpha). \tag{2.21}$$

The non-dimensional parameters are

$$\Lambda_L = \frac{9}{2}\left(\frac{L}{a}\right)^2, \quad Pe_L = \frac{U_s L}{D_C}, \quad Re_L = \frac{\rho_C \, U_s \, L}{\mu_C}. \tag{2.22}$$

With this scaling Λ_L and Pe_L measure the convective particle flux relative that due to shear-induced and Brownian diffusion of particles respectively. Λ_L also appears as the ratio of buoyancy and viscous forces. Zero mixture and particle flux conditions normal to the wall and no-slip conditions for the mixture fluid complete the formulation.

Regarding the particular choice of the non-dimensional diffusivity, $D(\alpha)$, one might think that the ability of the Brownian diffusion to prevent particles from reaching maximum packing relies on the assumption of an infinite value of $D(\alpha_m)$. However, since the settling rate decreases rapidly at high concentrations this is not the case. To see this, consider the one-dimensional model problem of a suspension settling due to gravity towards a horizontal plate, assuming an initially homogeneous volume fraction, α_0, and an initial height, h_0, of the suspension. One finds that the steady-state solution as $t \to \infty$ yields an implicit relation for the volume fraction at the wall, $\Pi_e(\alpha_w) = \alpha_0 \, U_s \, h_0/D_C$, where $\Pi_e(\alpha)$ is the effective non-dimensional osmotic pressure defined by $\Pi_e'(\alpha) = D(\alpha)/f(\alpha)$. A value of the volume fraction at the wall, α_w, that is less than the maximum packing limit, α_m, can thus be guaranteed for any particle load if $\Pi_e(\alpha)$ diverges as $\alpha \to \alpha_m$. Thus, it would be sufficient to require, say,

$$\Pi_e(\alpha_w) \geqslant \text{const.} \log{(\alpha_m - \alpha)^{-1}} \quad \text{as} \quad \alpha \to \alpha_m.$$

Using the definition of $\Pi_e(\alpha)$ above, the corresponding criterion for $D(\alpha)$ with a given choice of $f(\alpha)$ is then $D(\alpha) \geqslant \text{const.} f(\alpha)/(\alpha_m - \alpha)$. In our case $f(\alpha)$ from (2.6) and (2.9) is such that maximum packing is prevented if

$$D(\alpha) \geqslant \text{const.} (\alpha_m - \alpha) \quad \text{as} \quad \alpha \to \alpha_m,$$

i.e. even diffusivities approaching zero at maximum packing may be sufficient.

3. Analysis

Λ_L and the Péclet number, Pe_L, are typically very large parameters indicating a boundary layer character of the flow. As shown by N & A, for the case without Brownian diffusion, the sediment will appear in a sublayer at the wall of thickness $\delta \sim L\Lambda_L^{-1/3}$ where buoyancy is balanced by viscous forces and inertia may be neglected if $Re_L \ll \Lambda_L^{1/3}$. For that case a similarity law exists for the sublayer and for which the length of the plate, L, is completely arbitrary. In the present paper, as the effect of Brownian motion is added, a new characteristic length, D_C/U_s, appears as the typical thickness of an equilibrated layer of settled Brownian particles on a horizontal surface. The Brownian and shear-induced diffusional particle fluxes on the inclined plate are thus of the same order of magnitude if the length $D_C/(U_s \cos \phi) \sim \delta \sim L\Lambda_L^{-1/3}$, i.e. if the Péclet number based on plate length

$$Pe_L \sim \Lambda_L^{1/3} \gg 1, \tag{3.1}$$

which is the parameter regime studied here. This implies a characteristic length of the

plate $L = a/(U_s \cos \phi a/D_C)^3$ and no similarity law exists for the boundary layer. Inertia is still negligible in the sediment sublayer if

$$Re_L \Lambda_L^{-1/3} \sim \frac{Re_L}{Pe_L} = \frac{D_C}{\mu_c/\rho_C} \ll 1. \tag{3.2}$$

In analogy with the discussion by N & A this means that there will be an inertial outer layer in the homogeneous part of the suspension where the momentum, produced in the sediment layer, is brought to zero by viscous forces further away from the plate. Outside the boundary layers there is a hydrostatic force balance in the bulk with a weak secondary bulk flow due to the presence of the boundary layers. Here, we analyse only the thinner sediment layer adjacent to the plate.

Balance of viscous and buoyancy forces in the momentum equation and the mixture continuity equation imply that the magnitudes of the velocity components of the mixture are $u \sim \Lambda_L^{1/3}$, $v \sim 1$ in the boundary layer. New boundary layer variables are therefore introduced according to

$$\mathscr{u} = \frac{u}{\cos \phi \Lambda_L^{1/3}}, \quad \mathscr{v} = \frac{v}{\cos \phi}, \quad \mathscr{j}_x = \frac{j_x}{\cos \phi \Lambda_L^{1/3}}, \quad \mathscr{j}_y = \frac{j_y}{\cos \phi},$$

$$\mathscr{x} = x, \quad \mathscr{y} = y \Lambda_L^{1/3}. \tag{3.3\,a–f}$$

To lowest order, it then follows from (2.4) with (2.20) that

$$\mathscr{j}_x = \mathscr{u} - \Lambda_L^{-1/3} [\epsilon/(1+\epsilon \alpha)] \alpha f(\alpha) \tan \phi$$

so that in (2.20) we can replace u with j_x to lowest order. The same holds for the momentum equation to lowest order with this scaling. The problem can then be formulated in terms of $\mathscr{j}$ and α only. Accordingly,

$$\frac{\partial \mathscr{j}_x}{\partial \mathscr{x}} + \frac{\partial \mathscr{j}_y}{\partial \mathscr{y}} = 0, \tag{3.4\,a}$$

$$\frac{\partial}{\partial \mathscr{x}}(\alpha \mathscr{j}_x) + \frac{\partial}{\partial \mathscr{y}}(\alpha \mathscr{j}_y) = \frac{\partial}{\partial \mathscr{y}} [\alpha(1-\alpha)f(\alpha)] + \frac{9}{2} \frac{\partial}{\partial \mathscr{y}}$$

$$\times \left[\beta(\alpha) \left| \frac{\partial \mathscr{j}_x}{\partial \mathscr{y}} \right| \frac{\partial \alpha}{\partial \mathscr{y}} + \frac{\kappa(\alpha)}{\mu_e(\alpha)} \frac{\left| \frac{\partial \mathscr{j}_x}{\partial \mathscr{y}} \right|}{\frac{\partial \mathscr{j}_x}{\partial \mathscr{y}}} \frac{\partial}{\partial \mathscr{y}} \left(\mu_e(\alpha) \frac{\partial \mathscr{j}_x}{\partial \mathscr{y}} \right) \right] + \frac{\partial}{\partial \mathscr{y}} \left(D(\alpha) \frac{\partial \alpha}{\partial \mathscr{y}} \right) + O(\Lambda_L^{-1/3}), \tag{3.4\,b}$$

$$Re_L \Lambda_L^{-1/3} \cos \phi (1+\epsilon \alpha) \left(\mathscr{j}_x \frac{\partial \mathscr{j}_x}{\partial \mathscr{x}} + \mathscr{j}_y \frac{\partial \mathscr{j}_x}{\partial \mathscr{y}} \right) = (\alpha - \alpha_0) \tan \phi$$

$$+ \frac{\partial}{\partial \mathscr{y}} \left(\mu_e(\alpha) \frac{\partial \mathscr{j}_x}{\partial \mathscr{y}} \right) + O(\Lambda_L^{-1/3}), \tag{3.4\,c}$$

$$\frac{\partial P}{\partial \mathscr{y}} = -\Lambda_L^{-1/3} \epsilon(\alpha - \alpha_0) \cos \phi + O(\lambda_L^{-2/3}), \tag{3.4\,d}$$

where (3.4d) just states that P equals the ambient bulk pressure to lowest order. It should be pointed out that the boundary layer approximation requires that $\phi \gg \Lambda_L^{-1/3}$

or the scaling (3.3) is invalid; a steady-state formulation of the problem for $\phi \sim \Lambda_L^{-1/3}$ or smaller is thus not necessarily well posed. The boundary conditions are

$$j_x(y=0) = 0, \quad j_y(y=0) = 0,$$

$$\left\{ \alpha f(\alpha) + \frac{9}{2}\beta(\alpha) \left|\frac{\partial j_x}{\partial y}\right| \frac{\partial \alpha}{\partial y} + \frac{\kappa(\alpha)}{\mu_e(\alpha)} \frac{\left|\frac{\partial j_x}{\partial y}\right|}{\frac{\partial j_x}{\partial y}} \frac{\partial}{\partial y}\left(\mu_e(\alpha)\frac{\partial j_x}{\partial y}\right) + D(\alpha)\frac{\partial \alpha}{\partial y} \right\}\Bigg|_{y=0} = 0,$$

$$\frac{\partial j_x}{\partial y}(y \to \infty) \to 0, \quad \alpha(y \to \infty) \to \alpha_0. \quad (3.4e\text{--}i)$$

These equations, (3.4a–i), have no self-similar solution, as mentioned above, but nevertheless it is convenient to introduce a stream function according to

$$\Psi = \xi F(\xi, \eta), \quad \xi = x, \quad \eta = y/x^{1/3}, \quad (3.5)$$

where η is, except for a constant scaling factor, the similarity variable introduced by N & A. The velocity components are then given by

$$j_x = \frac{\partial \Psi}{\partial y} = \xi^{2/3} F_\eta, \quad j_y = -\frac{\partial \Psi}{\partial \xi} = -F + \frac{\eta}{3}F_\eta - \xi F_\xi, \quad (3.6)$$

where from here on subscripts will be used to indicate partial derivatives. If inertia is neglected the momentum equation (3.4c) to lowest order then reduces to

$$\tan\phi(\alpha - \alpha_0) + [\mu_e(\alpha)F_{\eta\eta}]_\eta = 0 \quad (3.7)$$

and (3.4b) yields the conservation of particles that

$$\xi(\alpha F_\eta)_\xi - (\alpha\xi F_\xi)_\eta - \alpha_\eta F = [\alpha f(\alpha)]_\eta$$
$$+ \frac{9}{2}\left[\beta(\alpha)|F_{\eta\eta}|\alpha_\eta + \frac{\kappa(\alpha)}{\mu_e(\alpha)}\frac{|F_{\eta\eta}|}{F_{\eta\eta}}(\mu_e(\alpha)F_{\eta\eta})_\eta\right]_\eta + \xi^{-1/3}[D(\alpha)\alpha_\eta]_\eta. \quad (3.8)$$

We also make the assumption $F_{\eta\eta} > 0$, which is confirmed by our results. The last equation is then suitably combined with (3.7):

$$\xi(\alpha F_\eta)_\xi - (\alpha\xi F_\xi)_\eta - \alpha_\eta F = \left[\alpha f(\alpha) - \frac{9}{2}\frac{\kappa(\alpha)}{\mu_e(\alpha)}\tan\phi(\alpha - \alpha_0)\right]_\eta$$
$$+ \tfrac{9}{2}[\beta(\alpha)F_{\eta\eta}\alpha_\eta]_\eta + \xi^{-1/3}[D(\alpha)\alpha_\eta]_\eta. \quad (3.9)$$

Thus, the shear-stress-induced migration mechanism does not appear as a diffusive term in (3.9) but rather as a contribution to the sedimentation flux which is then effectively smaller than $\alpha f(\alpha)$. The no-slip and zero-flux conditions at the wall imply

$$F(\xi, 0) = F_\eta(\xi, 0) = 0, \quad (3.10)$$

$$\left\{\alpha f(\alpha) - \frac{9}{2}\frac{\kappa(\alpha)}{\mu_e(\alpha)}\tan\phi(\alpha - \alpha_0) + \tfrac{9}{2}\beta(\alpha)F_{\eta\eta}\alpha_\eta + \xi^{-1/3}D(\alpha)\alpha_\eta\right\}\Bigg|_{\eta=0}. \quad (3.11)$$

In the outer part of the boundary layer the volume fraction should adjust to α_0 in the homogeneous suspension and the shear rate match the flow in the outer inertial layer which to lowest order just require that

$$F_{\eta\eta}(\xi, \eta \to \infty) \to 0. \quad (3.12)$$

The boundary layer equations above were solved numerically through a marching procedure down the plate, based on a scheme originally proposed by Harris & Blanchard (1982) for compressible boundary layers. One observes that if it were not for the last term in (3.9), due to Brownian diffusion, the equations would be of self-similar form, which is actually the motivation for the ansatz (3.5). The factor $\xi^{-1/3}$ in (3.9) indicates that far downstream on the plate the flow might actually approach self-similar behaviour. In fact, in the case of essentially non-Brownian particles the characteristic length L, used here, is indeed a small distance and the self-similar form of the equations would seem to be a good approximation. As we shall see, however, this is not always the case.

For small values of ξ the boundary layer scaling (3.5) is not relevant and equations (3.7), (3.9) are then not in an appropriate form to start the marching procedure at $\xi = 0$. Close to the leading edge the departure within the boundary layer from the ambient volume fraction is small and buoyancy forces a weak bulk flow balanced by viscous forces in (3.4c) implying $\alpha - \alpha_0 \sim j_x/\delta^2$, where δ is the boundary layer thickness in this region. The divergence of the particle flux constitutes a balance of convection with the bulk flow and Brownian diffusion, which is the overall dominant diffusion mechanism close to the edge; thus from (3.4b) $j_x/x \sim 1/\delta^2$. The ambient sedimentation flux towards the wall is cancelled by Brownian diffusion at the wall which by (3.4g) requires $(\alpha - \alpha_0)/\delta \sim 1$. One finds then that $\delta \sim x^{1/5}$ and the appropriate ansatz for $x \ll 1$ is

$$\Psi = \xi^{4/5}\mathscr{F}(\xi,\zeta), \quad \xi = x, \quad \zeta = y/x^{1/5}. \tag{3.13}$$

An approximate solution can then be obtained through expansions of the type

$$\mathscr{F}(\xi,\zeta) = \mathscr{F}_0(\zeta) + \xi^{1/5}\mathscr{F}_1(\zeta) + O(\zeta^{2/5}), \tag{3.14a}$$

$$\alpha(\xi,\zeta) - \alpha_0 = \xi^{1/5}\mathscr{A}_1(\zeta) + \xi^{2/5}\mathscr{A}_2(\zeta) + O(\xi^{3/5}). \tag{3.14b}$$

From descending orders of $\xi^{1/5}$ in the governing equations (3.7), (3.9) a system of ordinary differential equations was derived for the unknown functions of (3.14) for which the lowest-order balance equations are given by

$$\mathscr{A}_1(\zeta)\tan\phi + \mu(\alpha_0)\mathscr{F}_0(\zeta)''' = 0. \tag{3.15a}$$

$$\tfrac{1}{5}\mathscr{F}_0(\zeta)'\mathscr{A}_1(\zeta) - \tfrac{4}{5}\mathscr{F}_0(\zeta)\mathscr{A}_1(\zeta)' = D(\alpha_0)\mathscr{A}_1(\zeta)'', \tag{3.15b}$$

$$\mathscr{F}_0(0) = 0, \quad \mathscr{F}_0(0)' = 0, \quad \alpha_0 f(\alpha_0) + D(\alpha_0)\mathscr{A}_1(0)' = 0, \tag{3.15c–e}$$

$$\mathscr{F}_0(\zeta)'' \to 0, \quad \mathscr{A}_1(\zeta) \to 0 \quad \text{as} \quad \zeta \to \infty. \tag{3.15f, g}$$

After evaluation of the two-term expansion solution, (3.14), at a small but non-zero value of ξ, it was transformed into the original coordinates, (3.5), and then continued by the marching procedure for the full equations (3.7), (3.9). The results generally adjusted smoothly with the expansion solution if the transformation point was chosen at a distance $\xi \leqslant 0.0001$ depending on the particular case studied and were insensitive to the transformation point at larger values of ξ.

4. Discussion

We present results for two different cases here. In the first case we let $\kappa = 0$, i.e. particle migration due to gradients in shear stress is neglected. The shear-induced diffusion model is then identical to that of N & A and novel effects are expected only
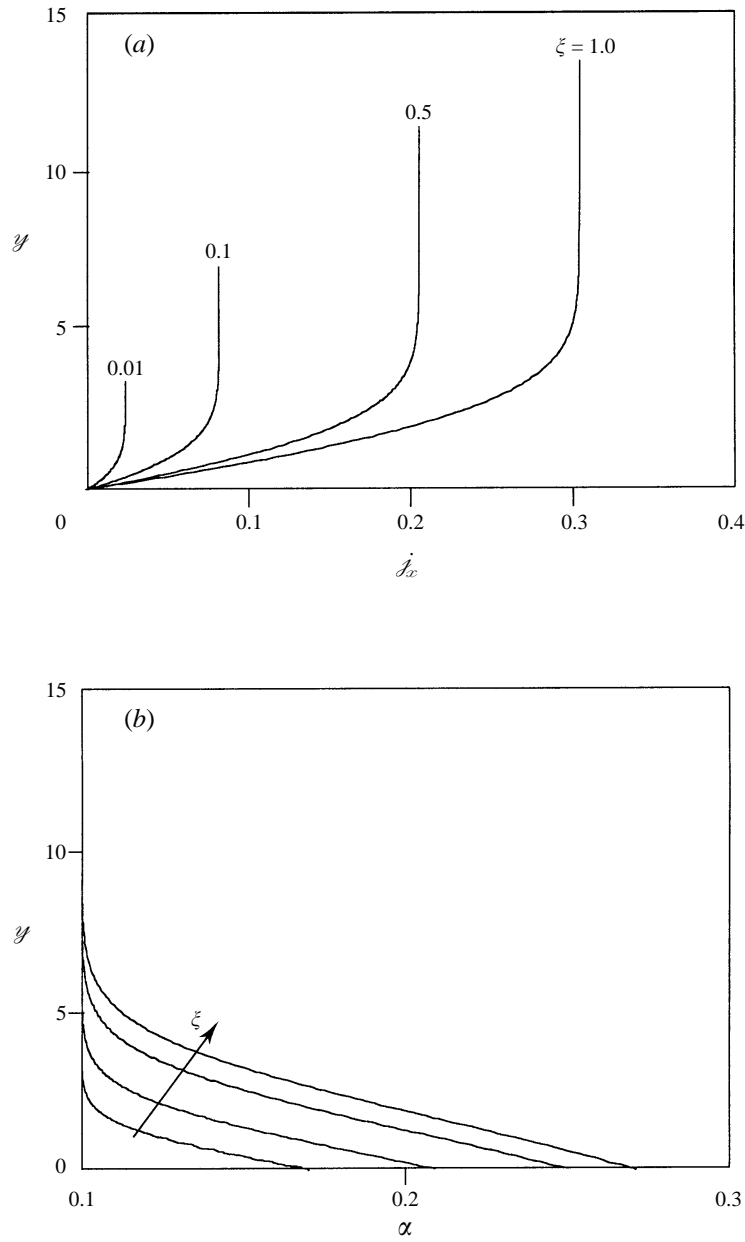
FIGURE 2. Boundary layer profiles of (*a*) mixture velocity, j_x, and (*b*) particle volume fraction, α, versus y for the case $\kappa = 0$ at $x = \xi = 0.01, 0.1, 0.5, 1.0$; $\alpha_0 = 0.1$, $\phi = 45°$.

due to Brownian diffusion. The migration model, with $\kappa \neq 0$, is included in the second case which differs from the study by K & A in that they allowed particle slip at the wall but no Brownian diffusion of particles.

Figure 2 shows the boundary layer profiles, versus y, of the mixture velocity, j_x, and particle volume fraction at various positions at the beginning of the plate for 45° inclination angle and $\alpha_0 = 0.1$ in the case $\kappa = 0$. Figure 3 shows the development further downstream; the boundary layer coordinate is here that defined in (3.5) and the mixture velocity is plotted as $F_\eta = j_x \xi^{-2/3}$. Close to the leading edge Brownian
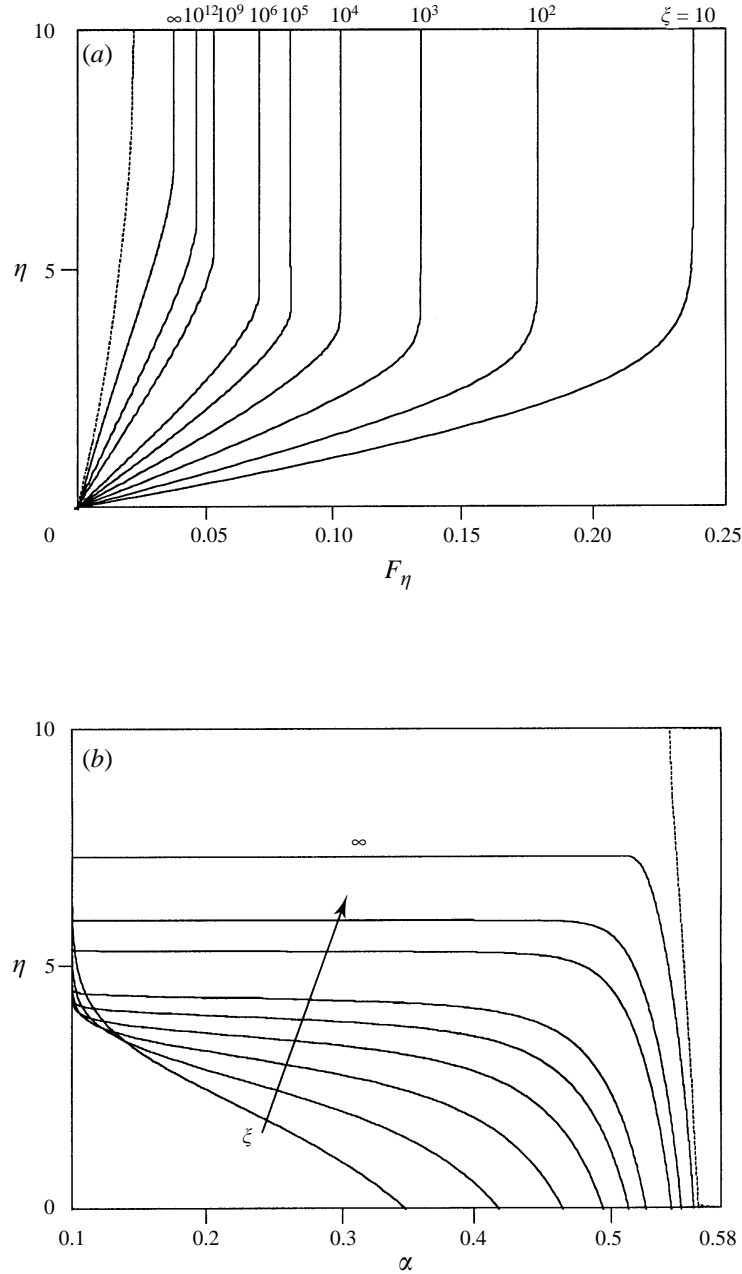
FIGURE 3. Boundary layer profiles of (*a*) the scaled mixture velocity, F_η, and (*b*) particle volume fraction, α, versus the boundary layer coordinate, η, for the case $\kappa = 0$ at $\xi = 10$, $i = 1, 2, 3, 4, 5, 6, 9, 12, \infty$; $\alpha_0 = 0.1$, $\phi = 45°$. -----, Corresponding similarity solution of N & A.

diffusion markedly dominates over the shear-induced diffusion with a characteristic exponential type of decay of the volume fraction away from the wall. Further downstream, as the boundary layer grows, shear-induced diffusion progressively overtakes as the dominant mechanism. However, in the outer part of the boundary layer, where the shear rate approaches zero, Brownian diffusion is still dominant and smooths the steepening profile of the concentration. The profile is truly smooth at the

boundary layer edge even for large, finite ξ, but the relative strength of the diffusivity is then so small that this structure is not visible in figure 3. In order to capture the very narrow shock structure at the edge of the boundary layer the numerical scheme uses a local refinement of the grid, following the location of the boundary layer edge.

The development of the wall-shear rate at $\alpha_0 = 0.1$ is shown for various inclination angles in figure 4. For large enough inclination angles the scaled shear rate, $F_{\eta\eta}(\xi, 0)$, asymptotically approaches a constant value far downstream which indicates self-similarity of the solution. If the inclination angle is too small, self-similarity is not approached, as can be seen for the lowermost curve in figure 4. However, a steady boundary layer solution is still available for the values of ξ considered in our computations.

A comparison of the boundary layer profiles at $\alpha_0 = 0.1$ for two values of ϕ, one of which does, and the other does not, allow approach to self-similarity far downstream, is shown in figure 5 at $\xi = 10^9$. At 45° inclination angle a substantial amount of shear is present in the near-wall region and Brownian diffusion is here essentially negligible. In this situation self-similarity is approached for large ξ. At 20° inclination angle, however, the body force on the sediment along the plate is not large enough to reproduce the shear rate required to counteract the packing of particles just by shear-induced diffusion. The sediment is then very close to maximum packing ($\alpha_m = 0.58$) at the wall with high viscosity and low shear rate. Brownian motion of the particles is here of vital importance since that alone apparently prevents them from reaching maximum packing. Further out in the boundary layer, where the shear rate is appreciable, shear-induced diffusion is also still the dominant mechanism for this smaller inclination angle. With these different balances within the layer self-similarity is not approached for large ξ and the boundary layer grows much faster than for the self-similar cases at larger inclination angles.

An insight into the particle flux balance at the wall may be obtained from (3.11) if $F_{\eta\eta}$ at the wall is expressed from the result of integrating (3.7), through the boundary layer and also $f(\alpha)$ is taken explicitly from (2.9):

$$\frac{1}{\mu_e(\alpha|_{\eta=0})}\left\{\alpha(1-\alpha) + \tfrac{9}{2}\tan\phi\,\beta(\alpha)\int_0^\infty (\alpha - \alpha_0)\,\mathrm{d}\eta\,\alpha_\eta + \xi^{-1/3}\mu_e(\alpha)\,D(\alpha)\,\alpha_\eta\right\}\Bigg|_{\eta=0} = 0. \quad (4.1)$$

Close to maximum packing, as the effective viscosity is large, the hindered settling velocity of the particles and the shear rate of the mixture are small. It then becomes clear that when ϕ is not large enough for the second term to balance the first one in (4.1), the last term may do so even if $\xi^{-1/3}$ is small. This effect is augmented by the diverging Brownian diffusivity at maximum packing but the above conclusion holds independently of this fact. As already discussed in §2 Brownian diffusion may prevent packing at α_m even if the diffusivity, under certain restrictions, were to approach zero as $\alpha \to \alpha_m$. Therefore, any choice of $D(\alpha)$, satisfying a restriction such as that given in §2, is expected to give results of roughly the same nature. Although the boundary layer growth, for cases of no self-similarity, have been found to grow much more rapidly, if for example, $D(\alpha_m)$ is finite rather than infinite as here, the overall qualitative picture is similar.

As a check on our computations for $\kappa = 0$ we compared the results far downstream on the plate with the self-similar solution obtained by N & A. Qualitatively the comparison was favourable but quantitatively the disagreement in boundary layer thickness or velocity and volume fraction at the boundary layer edge were up to 50 % as for example shown (dashed) for the case in figure 3. This obviously requires comment. A typical feature of the self-similar solution is that it involves a kinematic
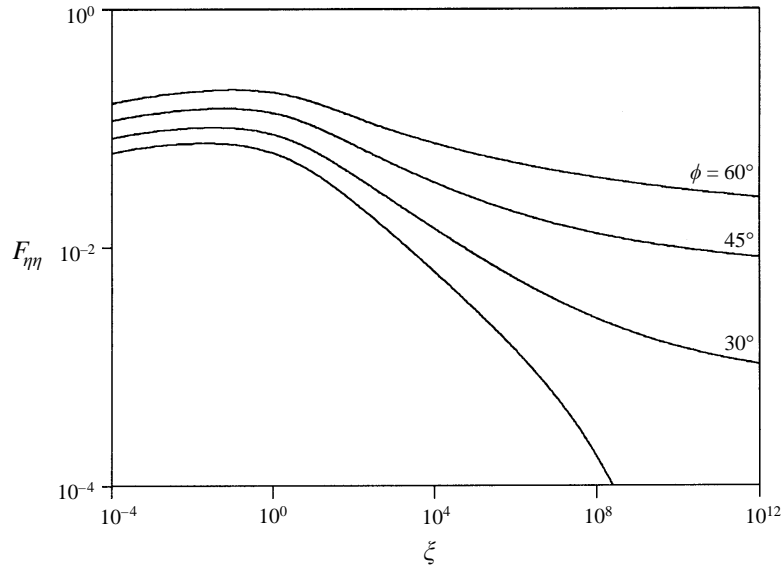
FIGURE 4. The scaled wall-shear stress, $F_{\eta\eta}(\xi,0)$, versus ξ for the case $\kappa = 0$ at various inclination angles $\phi = 20°$, $30°$, $45°$, $60°$; $\alpha_0 = 0.1$.
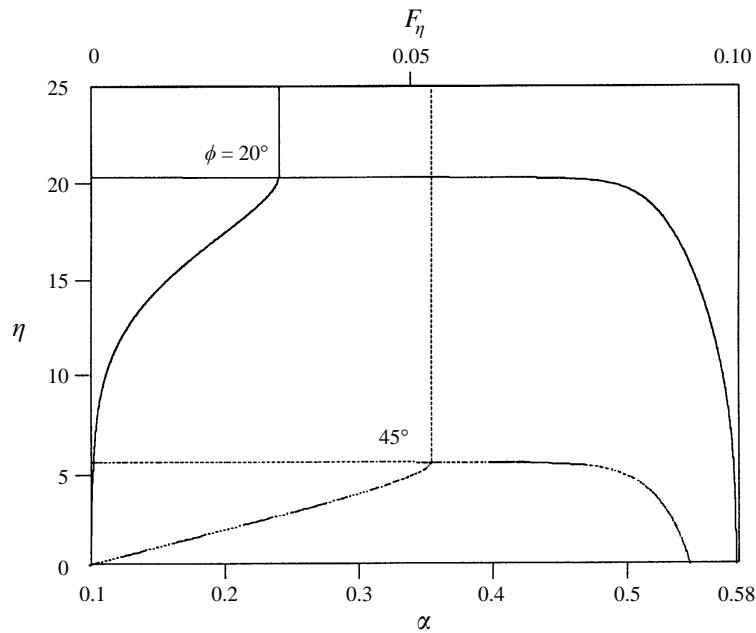

FIGURE 5. Comparison, for the case $\kappa = 0$, $\alpha_0 = 0.1$ at $\xi = 10^9$, of a boundary layer profile for $\phi = 45°$ which allows approach to self-similarity for large values of ξ, and one at $\phi = 20°$ that does not.

shock construction at the edge of the boundary layer. In our computations, this is not necessary since there will always be a small, but non-zero, diffusivity from the Brownian motion present that produces a continuous shock structure in its place. Apparently, the limit of very small diffusivity does not recover the expected self-similar solution found by N & A. One may see why this is so from the following physical
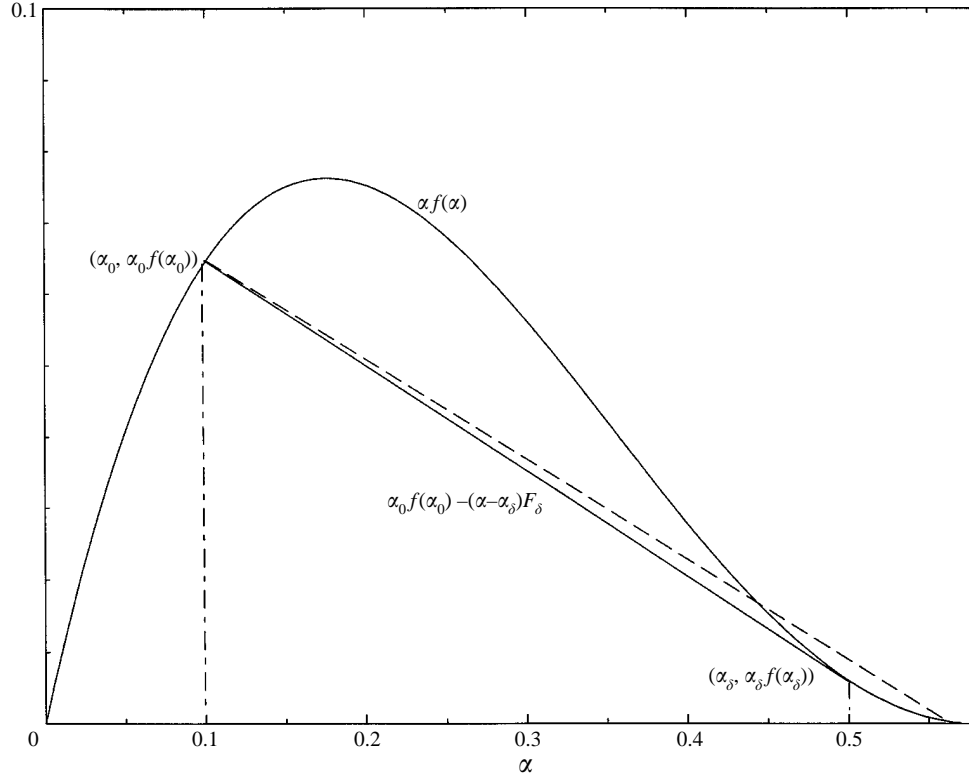
FIGURE 6. The drift flux curve, $\alpha f(\alpha)$, and the shock construction of the similarity solution. The dashed line indicates the shock construction used by N & A.

reasoning regarding the particle flux normal to the shock interface. For a non-diffusive solution, particle continuity across the steady shock requires

$$\alpha_\delta(f(\alpha_\delta) + F_\delta) = \alpha_0(f(\alpha_0) + F_\delta), \tag{4.2}$$

where α_0 and α_δ are the volume fractions on the upper and lower sides of the shock, F_δ is the downward fluid velocity normal to the shock and $f(\alpha)$ is the hindered particle velocity relative to that. Graphically (4.2) requires the slope of the secant between $(\alpha_0, \alpha_0 f(\alpha_0))$ and $(\alpha_\delta, \alpha_\delta f(\alpha_\delta))$ on the drift flux curve in figure 6 to be $-F_\delta$. Considering a diffusive model problem, with a ξ-independent artificial diffusivity $\nu \ll 1$, for which the volume fraction varies continuously between α_0 and α_δ, the particle flux balance within the shock structure is

$$\alpha\,(f(\alpha) + F_\delta) + \nu\,\frac{\mathrm{d}\alpha}{\mathrm{d}\eta} = \alpha_0(f(\alpha_0) + F_\delta); \quad \alpha_0 \leqslant \alpha \leqslant \alpha_\delta, \tag{4.3}$$

where $\nu\,\mathrm{d}\alpha/\mathrm{d}\eta$ is the diffusive particle flux (towards the wall). Since α decreases away from the wall the diffusive term is negative since the diffusivity, ν, is always a positive quantity. This with (4.3) and secondly by (4.2) implies the inequality

$$\alpha f(\alpha) \geqslant \alpha_0\,f(\alpha_0) - (\alpha - \alpha_0)\,F_\delta = \alpha_0\,f(\alpha_0) + (\alpha - \alpha_0)\,\frac{(\alpha_\delta\,f(\alpha_\delta) - \alpha_0\,f(\alpha_0))}{\alpha_\delta - \alpha_0}, \tag{4.4}$$

where equality holds for $\alpha = \alpha_0$ and $\alpha = \alpha_\delta$. As illustrated in figure 6, (4.4) requires the

drift flux curve, $\alpha f(\alpha)$, always to be above the secant between α_0 and α_δ, or otherwise a positive diffusivity could never establish a flux balance in the corresponding shock structure. (A more general and stringent derivation of (4.4) is given by Lax (1973).) Owing to the presence of an inflection point on the drift flux curve, the shock construction by N & A violates this requirement as indicated by the dashed line. We found, however, another self-similar solution with which our computations also agree quantitatively. Velocity and concentration profiles of the new similarity solution are seen as the last in the series of curves ($\xi \to \infty$) for the case shown in figure 3. This solution was obtained by using a modified shock construction as given by a stability requirement implicit in (4.4). In order for a kinematic shock to be an acceptable solution it must be stable to imposed infinitesimal disturbances; e.g. the shock must re-establish itself if it is slightly disturbed into a steep, but continuous, profile. Usually the flow through a shock is stable/evolutionary (see Landau & Lifshitz 1987, p. 10) if infinitesimal disturbances propagate into the shock on both sides but such a construction is not allowed here due to the inflection point in the drift flux curve $\alpha f(\alpha)$, the presence of which seems to be a general feature for a wide class of suggested hindered-settling functions. (For a description of different types of kinematic sedimentation waves see e.g. Wallis 1969, pp. 190–194.) Therefore, in addition to the usual kinematic shock relations for conservation of matter across the shock we imposed the condition (Wendroff 1972a, b)

$$\frac{\alpha_\delta f(\alpha_\delta) - \alpha_0 f(\alpha_0)}{\alpha_\delta - \alpha_0} - \frac{\mathrm{d}}{\mathrm{d}\alpha}(\alpha f(\alpha))\bigg|_{\alpha = \alpha_\delta} = 0, \tag{4.5}$$

which follows as the only possible limit of (4.4) as $\alpha \to \alpha_\delta$ in this case. Physically this means that imposed concentration disturbances, propagating as kinematic waves in the immediate neighbourhood of the shock, will be stationary at the lower side of the shock. On the other hand, a shock as constructed by N & A and similarly by K & A is unstable to small disturbances and would be disintegrated by expansion waves at the lower side of the shock. Their procedure is based on a regularity assumption for the solution as the shock wave is approached from below. The momentum and particle conservation equations may then be reduced to an algebraic equation for the variables at the lower side of the shock which actually states that the wave speed there is negative and away from the shock (equation (4.11) in N & A and equation (22) in K & A). As shown in the Appendix their regularity assumption does not hold if (4.5) is imposed. Graphically (4.5) states that the shock construction in figure 6 must be such that the secant is tangent to the drift flux curve at $\alpha = \alpha_\delta$ whereas the regularity assumption leads to a secant with larger negative slope than the drift flux curve at $\alpha = \alpha_\delta$. More details about the new self-similar solution are given in the Appendix where solutions to the diffusive model problem are also discussed.

The existence or non-existence of the new modified self-similar solution for various settings of the inclination angle and volume fraction α_0 gave qualitatively the same type of result as that found by N & A for steady self-similar solutions. As shown in figure 7, though, the curve above which self-similar steady-state solutions are available is displaced upwards. The new boundary is given by error bars only since it was determined from computations by the marching procedure like those in figure 4. (The integration of the similarity form of the equations presented an ill-conditioned iteration problem for the boundary layer thickness and two unknown parameter values at the wall and therefore could not be used for the purpose of determining the new curve in figure 7.) Note that this new curve represents the boundary between regions
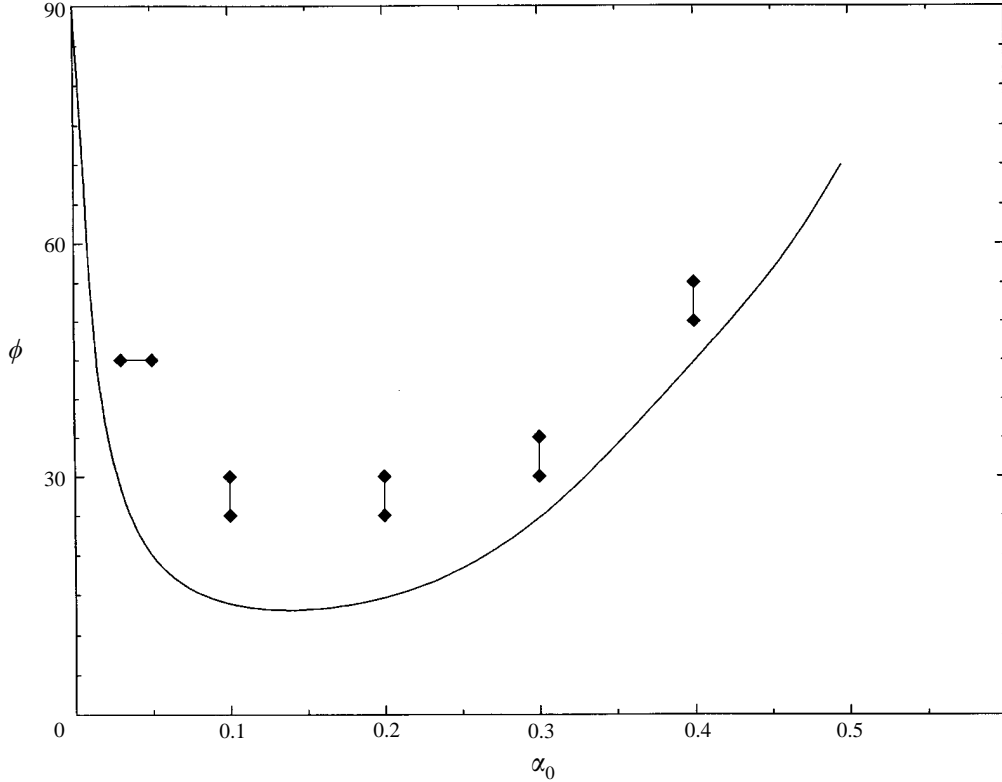
FIGURE 7. Curves above which self-similar solutions are available as given by N & A and by the present theory for $\kappa = 0$ (error bars).

where self-similarity is approached and not approached for large values of ξ, rather than a boundary between regions of steady and non-steady states. All our computations ($\phi \gg \Lambda_L^{-1/3}$) give steady results. Also, the shape of the boundary in figure 7 is of course completely independent of the Brownian diffusivity and is not affected by the particular model used for $D(\alpha)$.

One of the typical features for the case $\kappa = 0$ is that for very small volume fractions of the suspension, α_0, very large inclinations of the plate are required for the existence of a self-similar approach for large ξ. One also finds that the boundary layer thickness of the self-similar solution, when it exists, grows indefinitely as $\alpha_0 \to 0$ with a sediment approaching maximum packing. However, in our case this anomaly for $\alpha_0 \to 0$ appears only if, roughly, $\alpha_0 \xi \to \infty$ whereas if $\alpha_0 \xi \to 0$ a steady solution is still available, i.e. at a large but fixed value of ξ the limit of vanishing α_0 is unambiguous. From the approximate expansion procedure, (3.14), one may deduce that the boundary layer thickness is $\sim (\xi/\alpha_0)^{1/5}$, which still grows for vanishing α_0, but at the same time we have for the mixture velocity and the volume fraction that

$$\dot{\jmath}_x \sim \xi^{3/5} \alpha_0^{2/5}, \quad \dot{\jmath}_y \sim \alpha_0^{1/5}, \quad \alpha - \alpha_0 \sim \xi^{1/5} \alpha_0^{4/5}, \tag{4.6}$$

which imply that all these quantities approach zero if at least $\xi \alpha_0^{2/3} \to 0$. The inclusion of Brownian motion thereby relaxes somewhat the puzzling behaviour for vanishing volume fraction.

In the second case, $\kappa \neq 0$, as particle migration due to shear stress is included in the model, boundary layer profiles look qualitatively very much the same as for the first case but with an important exception. The odd behaviour of the self-similar solution
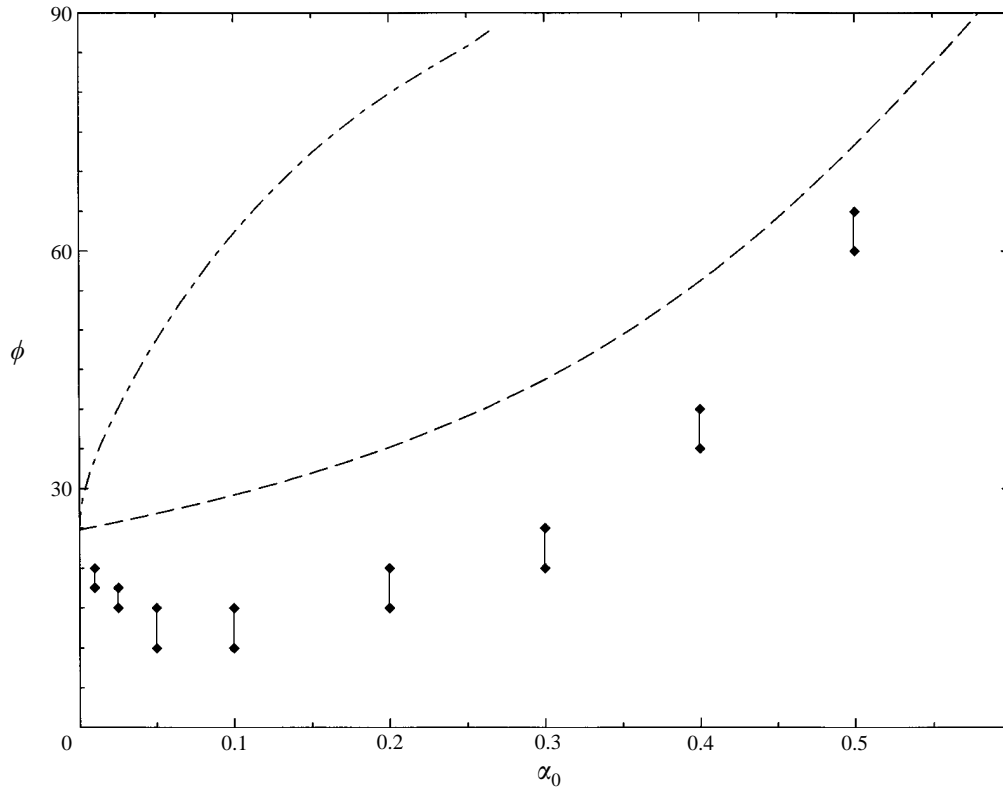
FIGURE 8. Region of available self-similar solutions for the case $\kappa \neq 0$ (error bars), the boundary for maximum packing limit at the wall as given by (4.8) (– – –), and the lower limit for constant volume fraction in the self-similar solution as given by (A 13) in the appendix (– · – · –).

for small volume fractions α_0 is not present. In this case, as is shown in figure 8, the boundary for the parameter region of approach to self-similarity gives a finite value of the inclination, $\phi < 90°$ as $\alpha_0 \to 0$, which was also found recently by K & A. Obviously, particle migration due to shear stresses alone may counteract the accumulation of particles in this limit. Investigating the particle flux balance at the wall, (4.1), in the case $\kappa \neq 0$ we get

$$\frac{1}{\mu_e(\alpha|_{\eta=0})}\left\{\alpha(1-\alpha)-\tfrac{9}{2}\tan\phi\kappa(\alpha)(\alpha-\alpha_0)\right.$$

$$\left.+\tfrac{9}{2}\tan\phi\beta(\alpha)\int_0^\infty (\alpha-\alpha_0)\,\mathrm{d}\eta\,\alpha_\eta+\xi^{-1/3}\mu_e(\alpha)\,D(\alpha)\,\alpha_\eta\right\}\Bigg|_{\eta=0} \quad 0, \quad (4.7)$$

which for a balance only between the two first terms would require the slope

$$\tan\phi = \frac{2}{9}\left\{\frac{\alpha(1-\alpha)}{\kappa(\alpha)(\alpha-\alpha_0)}\right\}\Bigg|_{\eta=0} \quad (4.8)$$

and where the limit for a self-similar solution to exist is obtained for maximum packing at the wall $\alpha(\eta=0)=\alpha_m$. This limit is shown, with $\alpha_m=0.58$, as a dashed line in figure 8 which at $\alpha_0=0$ gives $\phi=\arctan[\tfrac{10}{27}(1-\alpha_m)/\alpha_m^2]=24.8°$, quite close to the extrapolated true curve. In fact, a particularly simple form of the self-similar solution is available for the case $\kappa \neq 0$. The volume fraction is then constant in the sediment layer and so the first two terms of (4.7) balance each other exactly throughout the

whole layer. This is possible since the shear stress-induced migration of particles, which counteracts the settling in this case, is effectively of non-diffusive character in the buoyancy-driven flow considered. Thus the dashed line in figure 8 would seem to be a lower boundary for this type of similarity solution. As shown in the Appendix though, a second criterion for this constant-volume fraction solution is given by a stability condition analogous to that discussed above the case $\kappa = 0$, which yields a more restrictive condition for this type of solution given by the dot-dashed line in figure 8. Thus, in the region above the dot-dashed line of figure 8 the similarity solution available constitutes a particle flux balance between settling and shear-stress-induced migration only, whereas outside this region shear-induced diffusion is active as well. Also, as shown in the Appendix, the boundary layer thickness of the self-similar solution is finite and $\sim \alpha_0^{1/3}$ for small α_0 if $\kappa \neq 0$. A comparison with the study of K & A shows that similar to our case they find regions along the plate with different characteristics and scaling laws. In their solution, particle slip at the wall is of major importance close to the leading edge whereas far downstream slip is progressively weaker. On the other hand, their steady-state solution is available, as in N & A, only for certain combinations of ϕ and α_0. In our solution Brownian diffusion is dominant at the leading edge and becomes progressively less important far downstream except at the boundary layer edge. For some values of ϕ and α_0 Brownian diffusion is also dominant far downstream as the sediment near the wall is close to maximum packing. Analogous to the case $\kappa = 0$ discussed previously this behaviour yields steady-state solutions for the parameter regime that was not available for the model used by K & A. Finally, the type of unstable shock construction used by N & A is also present in K & A, implying that a possible unifying limit of non-Brownian particles from our solution and particles without slip at the wall from the K & A solution would not give exactly the same result.

5. Conclusions

We considered continuous, steady settling of Brownian particles on an inclined plate and the accompanied buoyancy-driven motion of the accumulated sediment. Also incorporated in the model was the diffusion of particles due to shear-induced hydrodynamic interaction. It was found that at the beginning of the plate, within a distance $\sim a[3kT/(4\pi a^3 \epsilon \rho_C g a \cos \phi)]^3$, Brownian motion is the dominating diffusion mechanism and effectively counteracts packing of particles in the sludge layer. Further downstream, where the sediment is thicker, shear-induced diffusion of particles may gradually become the most dominant contribution. If the inclination of the plate is too small though, the shear rate does not grow large enough to suspend the particles through the whole sediment layer. Instead, in a region close to the wall, Brownian motion of the particles prevents the packing from reaching its maximum at which, otherwise, all motion would cease.

We were also able to resolve an issue raised by Nir & Acrivos (1990) who found that no steady-state solution to this problem was available in the limit of vanishing volume fraction, α_0, above the sediment, since in their case the thickness of the sludge grows indefinitely and the particle packing in the sediment approaches its maximum as $\alpha_0 \rightarrow 0$. Here, with the additional effect of Brownian motion, this non-intuitive behaviour did not appear if the limit of vanishing α_0 was considered for a finite fixed length of the plate. Moreover, if the hydrodynamic particle interaction was complemented with a model for particle migration due to gradients in shear stress, the limit $\alpha_0 \rightarrow 0$ gave physically acceptable results even in the limits of vanishing Brownian motion.

For the reconsidered problem of zero Brownian motion, we found that the shock condition must be complemented with a requirement of zero kinematic-wave speed, locally at the lower side of the shock, or this solution would not be the same as that for the limit of vanishing Brownian diffusivity in our extended formulation. In fact, the inclusion of an artificial Brownian diffusivity as a means of smoothing concentration shocks is also justified because of the failure of the continuum approximation at a length scale of the particle diameter. In this respect, it is a requisite of the non-Brownian self-similar solution to be insensitive to the presence of a small non-zero diffusivity.

In summary, the present theory allows a steady-state solution for any volume fraction above the sediment and any choice of inclination angle much larger than $[\epsilon \rho_C ga^4/kT]^2 \ll 1$. Essentially the same regions of parameter space as those given by Nir & Acrivos (1990) and Kapoor & Acrivos (1995) for available steady states are in our cases regions for which far downstream on the plate Brownian diffusion appears negligible compared to shear-induced diffusion and particle migration due to shear stress gradients.

Appendix. The self-similar solution

The self-similar form of the equations is obtained in the limit $\xi \to \infty$ for which all ξ-derivatives are zero in equation (3.9). The governing equations are then

$$\tan\phi(\alpha - \alpha_0) + [\mu_e(\alpha)F'']' = 0, \tag{A 1}$$

$$-\alpha'F = \left[\alpha f(\alpha) - \frac{9}{2}\frac{\kappa(\alpha)}{\mu_e(\alpha)}\tan\phi(\alpha - \alpha_0)\right]' + \tfrac{9}{2}[\beta(\alpha)F''\alpha']', \tag{A 2}$$

where at the wall we have

$$F(0) = F'(0) = 0, \tag{A 3}$$

$$\left\{\alpha f(\alpha) - \frac{9}{2}\frac{\kappa(\alpha)}{\mu_e(\alpha)}\tan\phi(\alpha - \alpha_0) + \tfrac{9}{2}\beta(\alpha)F''\alpha'\right\}\Big|_{\eta=0}. \tag{A 4}$$

In the self-similar case the sediment has a well-defined thickness, δ say, with edge boundary conditions

$$F''(\delta) = 0, \quad \alpha(\delta) = \alpha_\delta, \quad F(\delta) = F_\delta. \tag{A 5a–c}$$

The values of α_δ and F_δ are determined by different procedures depending on the values of α_0 and ϕ and we also consider the cases $\kappa = 0$ and $\kappa \neq 0$ separately.

For $\kappa = 0$ the sedimentation drift flux is just $\alpha f(\alpha)$. This function has an inflection point at $\alpha = \alpha_{in} = 0.352$. If $\alpha_0 < \alpha_{in}$ a kinematic shock in the volume fraction appears at the edge of the sediment layer for which the conservation of particles across the shock yields

$$\frac{\alpha_\delta f(\alpha_\delta) - \alpha_0 f(\alpha_0)}{\alpha_\delta - \alpha_0} = -F_\delta. \tag{A 6}$$

Due to the inflection point of the drift flux curve the shock construction is complemented by the tangent condition

$$\frac{\alpha_\delta f(\alpha_\delta) - \alpha_0 f(\alpha_0)}{\alpha_\delta - \alpha_0} = \frac{\mathrm{d}}{\mathrm{d}\alpha}(\alpha f(\alpha))\Big|_{\alpha=\alpha_\delta}, \tag{A 7}$$

which must be applied whenever the shock tends to be disintegrated by expansion

waves. In the case $\alpha_0 > \alpha_{in}$, no shock appears and $\alpha_\delta = \alpha_0$. An equation for F_δ is in this case obtained by eliminating the rational expression between (A 6) and (A 7). The position of the shock, δ, must for any α_0 be determined as a part of the integration procedure.

Even though the form of (A 2) is not that of a kinematic wave equation, shocks may still appear in the solution, for $\alpha_0 < \alpha_{in}$, since the diffusivity approaches zero at the edge of the sediment. Locally at the edge the particle flux balance is therefore similar to a kinematic wave problem. To justify the use of (A 6) and (A 7), taken from kinematic wave theory, we may investigate the particular behaviour of the solution close to the shock and verify that a solution of this form exists. By an expansion of (A 2) as $\eta \to \delta$ from below and using (A 6), (A 7) we obtain

$$\alpha - \alpha_\delta = \frac{A}{\log{(B/(\delta-\eta))}}, \quad \alpha' = -\frac{(\alpha-\alpha_\delta)^2}{(\delta-\eta)\,A}, \quad F'' = (\delta-\eta)\,(\alpha_\delta-\alpha_0)\,\frac{\tan\phi}{\mu(\alpha_\delta)}, \quad \text{(A 8)}$$

where

$$A = \tfrac{9}{2}\beta(\alpha_\delta)\,(\alpha_\delta-\alpha_0)\,\frac{\tan\phi}{\mu(\alpha_\delta)}\,\frac{2}{(\mathrm{d}^2/\mathrm{d}\alpha^2)\,[\alpha f(\alpha)]_{\alpha=\alpha_\delta}}, \quad \text{(A 9)}$$

and B is a constant which can be determined by matching to the complete solution. Thus, approached from below, the volume fraction of the self-similar solution has infinite derivative at the edge of the sediment and, although the diffusive particle flux approach zero at the shock, (A 2) shows an intricate balance involving all terms. The assumption imposed by N & A and likewise by K & A that terms like $(\alpha')^2 F''$ and $\alpha'' F''$ in (A 1), (A 2) vanish as the shock is approached from below is thus incorrect and results in unstable shock constructions in their cases, as discussed in §4.

To confirm the asymptotic approach, for large ξ, of the full non-similar solution to the self-similar one we found that extremely large values of ξ are required. In fact, it was not practical any longer to use the marching procedure for the boundary layer. We therefore solved (A 2) with a small constant artificial diffusivity, ν_{art}, replacing the true Brownian diffusivity. The equations are then still of self-similar form and no marching is needed. Instead, the equations were solved for decreasing values of the artificial diffusivity. A series of profiles from these calculations is shown in figure 9 together with the self-similar solution for $\alpha_0 = 0.1$, $\phi = 45°$. The reason for the slow approach is due to the logarithmic type of behaviour, (A 8), close to the shock. One may show that the shock-structure solution for small artificial diffusivity has an approach to the outer solution of the same form as (A 8) with $B \sim \nu_{art}$, which indicates that indeed the solution varies slowly with ν_{art}.

For the case $\kappa \neq 0$ similar arguments for the appearance of a kinematic shock hold if the effective drift flux is replaced by the full expression in the first bracket of (A 2) with $\kappa(\alpha)$ according to (2.11 b). Characteristic for this case is that for some values of α_0 and ϕ a particularly simple form of the solution is available. The volume fraction is then constant, $\alpha = \alpha_w$, through the whole sediment and determined from the boundary condition at the wall (A 4) with $\alpha' = 0$. With $f(\alpha)$ given explicitly by (2.9) this yields

$$\frac{1}{\mu_e(\alpha_w)}\{\alpha_w(1-\alpha_w) - \tfrac{9}{2}\tan\phi\,\kappa(\alpha_w)\,(\alpha_w-\alpha_0)\} = 0. \quad \text{(A 10)}$$

One may note here that any solution $\alpha_w(\phi, \alpha_0) \neq \alpha_m$ of (A 10) is independent of the effective viscosity law used. The velocity profile is then integrated directly from (A 1):

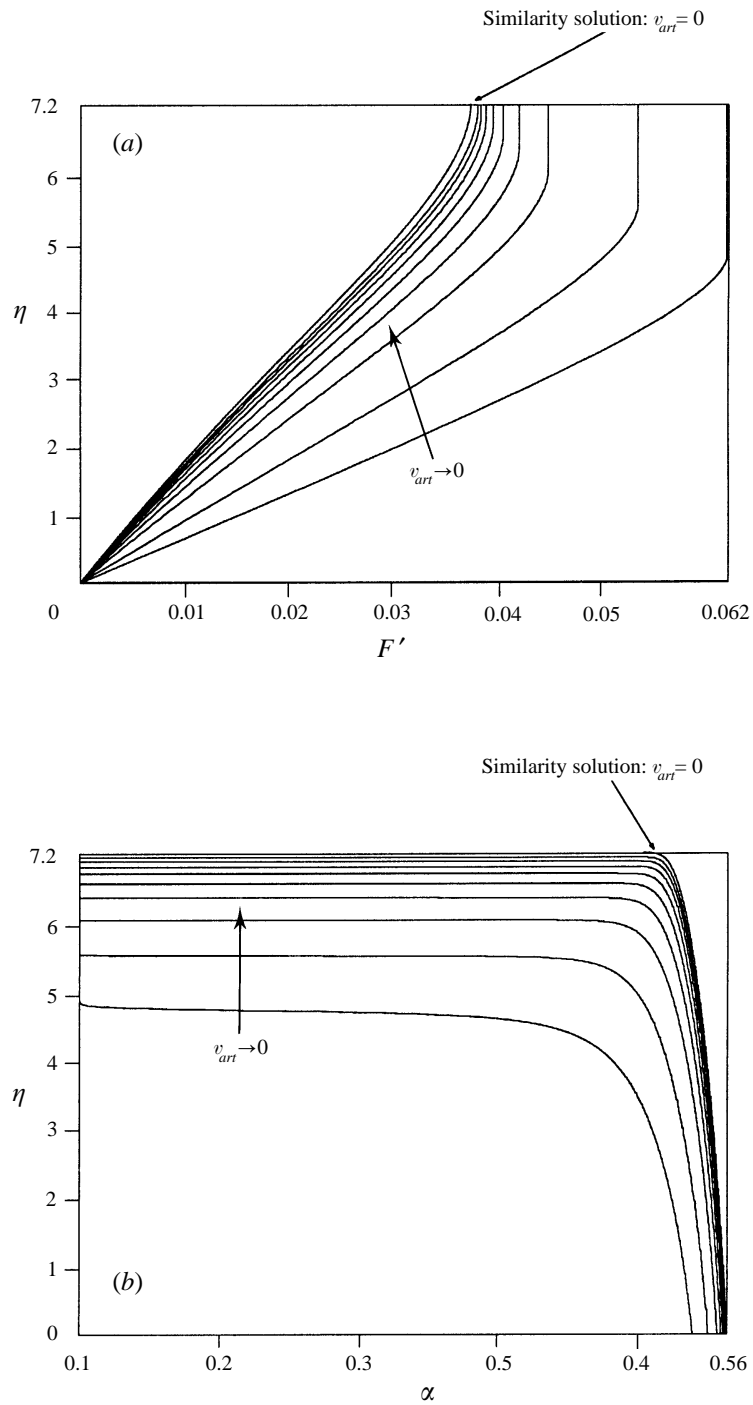$$F' = \frac{\tan\phi}{\mu_e(\alpha_w)}\,(\alpha_w-\alpha_0)\,\eta(\delta-\eta/2), \quad \text{(A 11)}$$

FIGURE 9. Approach to the self-similar solution for vanishing diffusivity, ν_{art}, in the case $\kappa = 0$ at $\alpha_0 = 0.1$, $\phi = 45°$. $\nu_{art} = 10^{-p}$, $p = 2, 3, \ldots, 10$. (*a*) Velocity profile, (*b*) particle volume fraction.

and the thickness of the sediment, δ, is determined from the shock condition (A 6) using the modified drift flux expression discussed above:

$$\delta = \left[\frac{3}{\tan\phi} \frac{\alpha_0(1-\alpha_0)}{(\alpha_w - \alpha_0)^2} \frac{\mu_e(\alpha_w)}{\mu_e(\alpha_0)} \right]^{1/3}. \tag{A 12}$$

A prerequisite for this solution to hold is two-fold: α_w is less than the maximum packing limit α_m; the shock construction is stable, i.e. the wave speed at the lower side of the shock is positive

$$-F_\delta(\phi, \alpha_0) - \frac{\mathrm{d}}{\mathrm{d}\alpha}\left[\alpha f(\alpha) - \frac{9}{2}\frac{\kappa(\alpha)}{\mu_e(\alpha)}\tan\phi(\alpha - \alpha_0) \right]\Bigg|_{\alpha = \alpha_\delta = \alpha_w(\phi, \alpha_0)} \geqslant 0. \tag{A 13}$$

Both criteria give a restriction on the combined choice of ϕ and α_0, explicitly obtained from (4.8) with $\alpha = \alpha_m$ and (A 13) respectively which are shown graphically in figure 8. The condition on the wave speed is seen to be the more restrictive one so that (A 13) actually implies $\alpha_w \leqslant \alpha_m$. (The wave speed at the upper side of the shock of this solution can be shown to be unconditionally negative as required.) Regarding the particularly interesting limit of vanishing α_0 one may see that (A 13) is fulfilled if

$$\alpha_0 \leqslant \alpha_w(\phi, 0)\,(2 - \alpha_w(\phi, 0))/(1 + \mu_e(\alpha_w(\phi, 0))), \tag{A 14}$$

where

$$\alpha_w(\phi, 0) = \frac{1}{5.4\tan\phi}[(1 + 10.8\tan\phi)^{1/2} - 1], \quad \phi \geqslant 24.8°. \tag{A 15}$$

Thus, the existence of the self-similar solution for $\kappa \neq 0$ at small α_0 is confirmed by this simple form of the solution.

REFERENCES

ACRIVOS, A., MAURI, R. & FAN, X. 1993 Shear-induced resuspension in a Couette device. *Intl J. Multiphase Flow* **19**, 797–802.

AUZERAIS, F. M., JACKSON, R. & RUSSEL, W. B. 1988 The resolution of shocks and the effects of compressible sediments in transient settling. *J. Fluid Mech.* **195**, 437–462.

BATCHELOR, G. K. 1976 Brownian diffusion of particles with hydrodynamic interactions. *J. Fluid Mech.* **74**, 1–29.

CHAPMAN, B. K. & LEIGHTON, D. T. 1991 Dynamic viscous resuspension. *Intl J. Multiphase Flow* **17**, 469–483.

DAVIS, R. H. & SHERWOOD, J. D. 1990 A similarity solution for steady-state cross-flow microfiltration. *Chem. Engng Sci.* **45**, 3203.

ECKSTEIN, E. C., BAILE, D. G. & SHAPIRO, D. G. 1977 Self-diffusion of particles in shear flow of a suspension. *J. Fluid Mech.* **79**, 191–208.

GADALA-MARIA, F. A. 1979 The rheology of concentrated suspensions. PhD thesis, Stanford University.

HARRIS, J. E. & BLANCHARD, D. K. 1982 Computer program for solving laminar, transitional, or turbulent compressible boundary-layer equations for two-dimensional and axisymmetric flow. *NASA Tech. Mem.* 83207.

ISHII, M. 1975 *Thermo Fluid Dynamic Theory of Two-Phase Flow*. Eyrolles, Paris.

ISHII, M. & CHAWLA, T. C. 1973 A generalised approach to the fluid dynamics of particulate systems. *Chem. Engng J.* **5**, 171–189.

KAPOOR, B. & ACRIVOS, A. 1995 Sedimentation and sediment flow in settling tanks with inclined walls. *J. Fluid Mech.* **290**, 39–66 (referred to herein as K & A).

KOCH, D. L. 1989 On hydrodynamic diffusion and drift in sheared suspensions. *Phys. Fluids* A **1**, 1742–1745.

LANDAU, L. D. & LIFSHITZ, E. M. 1987 *Fluid Mechanics*. 2nd Edn. Pergamon Press.

LAX, P. D. 1973 Hyperbolic systems of conservation laws and the mathematical theory of shock waves. *SIAM Regional Conf. Series in Appl. Math.* No. 11.

LEAL, L. G. 1973 *Chem. Engng Commun.* **1**, 21.

LEIGHTON, D. & ACRIVOS, A. 1986 Viscous resuspension. *Chem. Engng Sci.* **41**, 1377–1384.

LEIGHTON, D. & ACRIVOS, A. 1987a Measurement of shear-induced self-diffusion in concentrated suspensions of spheres. *J. Fluid Mech.* **177**, 109–131.

LEIGHTON, D. & ACRIVOS, A. 1987b The shear-induced migration of particles in concentrated suspensions. *J. Fluid Mech.* **181**, 415–439.

NIR, A. & ACRIVOS, A. 1990 Sedimentation and sediment flow on inclined surfaces. *J. Fluid Mech.* **212**, 139–153 (referred to herein as N & A).

SCHAFLINGER, U. 1996 Laminar transport of solid particles suspended in liquids. In *The Flow of Particles in Suspensions* (ed. U. Schaflinger). Springer.

SCHAFLINGER, U., ACRIVOS, A. & ZANG, K. 1990 Viscous resuspension of a sediment within a laminar and stratified flow. *Int J. Multiphase Flow* **16**, 567–578.

WALLIS, G. B. 1969 *One-dimensional Two-phase Flow*. McGraw-Hill.

WENDROFF, B. 1972a *J. Math. Anal. Appl.* **38**, 454.

WENDROFF, B. 1972b *J. Math. Anal. Appl.* **38**, 640.

WOODCOCK, L. W. 1981 Glass transition in the hard-sphere model and Kauzmann's paradox. *Ann. NY Acad. Sci.* **37**.